computation

MDPI

Article

Serial DF Relayed FSO Links over Mixture Gamma Turbulence Channels and Nonzero Boresight Spatial Jitter

Nikolaos A. Androutsos [1], Hector E. Nistazakis [1,*], Hira Khalid [2], Sajid S. Muhammad [2] and George S. Tombras [1]

[1] Department of Electronics, Computers, Telecommunications and Control, Faculty of Physics, National and Kapodistrian University of Athens, 15784 Athens, Greece

[2] Department of Electrical Engineering, National University of Computer and Emerging Sciences, Block B, Faisal Town, Lahore, Islamabad 44000, Pakistan

* Correspondence: enistaz@phys.uoa.gr; Tel.: +30-210-7276710

Received: 30 April 2019; Accepted: 1 July 2019; Published: 5 July 2019

Abstract: Over the past few years, terrestrial free space optical (FSO) communication systems have demonstrated increasing research and commercial interest. However, due the signal's propagation path, the operation of FSO links depends strongly on atmospheric conditions and related phenomena. One such significant phenomenon is the scintillation caused by atmospheric turbulence effects; in order to address the significant performance degradation that this causes, several statistical models have been proposed. Here, turbulence-induced fading of the received optical signal is investigated through the recently presented mixture Gamma distribution, which accurately describes the irradiance fluctuations at the receiver's input of the FSO link. Additionally, at the same time, it significantly reduces the mathematical complexity of the expressions used for the description of composite channels with turbulence along with nonzero boresight pointing error-induced fading. In order to counterbalance the performance mitigation due to these effects, serial decode-and-forward relays are employed, and the performance of the system is estimated through derived mathematical expressions.

Keywords: FSO communication systems; mixture gamma distribution model; DF relays; pointing errors with nonzero boresight

1. Introduction

Free Space Optical (FSO) communication uses laser beams for the wireless transmission of data. In these systems, light is emitted from the transmitter and propagates towards a photodiode in the receiver side through the atmosphere. This technology has now emerged as a reliable alternative to Radio Frequency (RF) or Millimeter Wave (MMW) systems in cases where point to point connections are required [1]; it is a practical technology that can counterbalance bottleneck connectivity problems [2]. Additionally, FSO communication can be a supplement to conventional RF or microwave links [2]. Over last decade, there has been an increase in commercial and research interest for FSO systems, because of the many advantages they have compared with classical RF systems. The most important of these are the high band with access, security, the low installation and operation costs and their operation in the unlicensed spectrum. Nevertheless, as for every wireless communication system, their operation depends strongly on the state of the channel, which is affected from atmospheric phenomena and conditions in the area between the transmitter and the receiver. Hence, one of the most significant performance mitigation factors of these systems is the atmospheric turbulence effect, which, for a typical outdoor line-of-sight (LOS) optical link, may cause rapid fluctuations of the irradiance at the

receiver side. Thus, the atmospheric channel has random time-varying characteristics because of the so-called scintillation effect which arises due to atmospheric turbulence, [1,3–11].

More analytically, the turbulence effect arises because of refractive index fluctuations of the atmosphere which occur due to pressure changes and temperature inhomogeneities. These variations result in eddies cells or air packets with variable sizes which act like refractive prisms of different sizes [1,12]. The interaction between these and the propagating laser beam generates random amplitude and phase fluctuations, which causes the well-known scintillation effect, as well as other minor effects such as beam wandering, beam spreading and beam break-up [12,13]. This, in turn, results in intensity fluctuations on the receiver side which degrade the performance of FSO systems. The intensity of these fluctuations in the propagating optical beam may be described by Rytov variance $\sigma_R^2 = 1.23 C_n^2 k^{7/6} L^{1/6}$, where C_n^2 is the refractive index structure parameter which describes the atmospheric turbulence strength, L is the length of the path, and $k = 2\pi/\lambda$ is the wavenumber, with λ being the wavelength [13]. The Rytov variance expression is valid in weak to moderate fluctuation regimes, and more precisely, week fluctuations characterized by $\sigma_R^2 < 1$, while moderate conditions are associated with $\sigma_R^2 \cong 1$. Strong fluctuation regimes are often more complicated and require special techniques in order to be implemented in FSO systems, which are not considered in our model [13].

Many statistical distribution models have been proposed for the description of the intensity fluctuations which arise from the scintillation effect. Each properly describes the scintillation effect caused by different turbulence strength, i.e., weak, moderate or strong, [12,14–17]. More precisely, lognormal and gamma statistical distributions are useful for describing the scintillations caused by weak turbulence, while GG, Malaga (M) and I-K are commonly used for a range from weak to strong turbulence conditions; finally, K and NE are suitable for strong and saturated conditions, respectively, [11,12,14,18–30]. In this work, as it will be shown below, the NE and GG distributions are approximated through the mixture Gamma (MG) distribution model [19,20,24].

MG distribution is a recently presented model which can accurately emulate many of the well-known distributions which are used for the scintillation effect, such as the gamma-gamma, the negative exponential, etc. [19,24]. Thus, it can be used either for weak to moderate or strong turbulence conditions. Additionally, the MG model has the significant advantage of being expressed through a mathematical expression for its probability density function (PDF) with relatively low complexity [19,20]. It may therefore be concluded that the obtained performance equations for the FSO link can be easily used in order to produce results for the design and implementation of workable FSO links. Additionally, the sways of high-rise buildings, in which the FSO terminals are usually located, due to wind loads, weak earthquakes, or thermal expansions, result in misalignment-induced fading of the received irradiance, which is known as the pointing errors effect [15,31,32]. The pointing errors effect consists of two components; the first is the boresight, which describes the fixed displacement between the beam center and the center of the detector, while the second is jitter. Jitter is the random offset of the beam center at the detector plane as given from the boresight [18,33]. Here, contrariwise to [34], we adopt a generalized misalignment fading model which takes also into account a nonzero boresight impact [12,18].

In order to combat the limitations associated with fading, relay-assisted FSO communication is an effective method to extend coverage and performance [15,35]. In [36], the MG model is adopted for the estimation of the performance of a SIMO FSO system with receivers' diversity, operating under the composite impact of nonzero boresight pointing errors and turbulence-induced scintillation fading. However, in this work, we investigate a totally different architecture and MG approximation is used for the study of another significant issue which concerns the way in which the effective radius of the FSO links can be extended.

More precisely, we investigate the performance of a serial DF-relayed FSO system with scintillation effect caused by atmospheric turbulence, along with a nonzero boresight pointing errors (NZB-PE) effect. Furthermore, in order to reduce the mathematical complexity of the widely adopted composite models used for the performance estimation in FSO systems operating under composite irradiance

channels, we adopt the MG model for the approximation of turbulence-induced scintillation fading [19]. Additionally, intensity modulation/direct detection (IM/DD) with On-Off Keying Modulation (OOK), or *L*-Pulse Position Modulation (*L*-PPM) schemes, are assumed. It should be mentioned here that the IM/DD scheme is one of the most common modes of detection in FSO systems. In DD, the receiver detects the instantaneous power of the impinged optical radiation on the photo-detector. Thus, the signal's intensity is modulated in order to carry digital information; the photo-detector's output is proportional to the received intensity. Note that the implementation of a DD scheme is simpler than other configurations, and thus, preferable for FSO systems with intensity modulation [12].

On the one hand, OOK is the most widely adopted and simplest modulation scheme that has been used in experimental and commercial FSO communication systems because of its ease in implementation with a simple receiver design, its bandwidth efficiency, and cost effectiveness. On the other hand, *L*-PPM does not require any decision threshold dependent on the input power (in contrast to OOK). It is also more power efficient, but more complex, and shows a rapid reduction of bandwidth efficiency [12,37]. In this respect, we derive mathematical expressions for the estimation of outage probability (OP) and average bit error rate (ABER) of the serially-DF-relayed FSO system.

The remainder of the work is organized as follows. In Section 2, we introduce the channel model comprising the scintillation effect and NZB-PE sub-models, respectively. Next, in Section 3, we proceed to the performance analysis of the DF-relayed FSO system in terms of the OP and the ABER, while the corresponding numerical results are presented in Section 4. Finally, some concluding remarks are presented in Section 5.

2. Channel Model

In this work, a DF FSO relay-assisted system is considered, in which the source transmits the information signal towards the receiver across H serial paths, and consequently, across the (H-1) DF relay nodes. All of the H paths have the same length, D, and each relay node, after receiving the signal, decodes it and retransmits it to the next relay, or to the final node, i.e., the receiver [15,38] of the FSO system. Furthermore, we consider an OOK with IM/DD scheme, and the received signal at the *h-th* hop, y_h, is given as [15,35,38]:

$$y_h = \eta I_h x_h + n_h, \tag{1}$$

where h represents the serial hops of the system, i.e., h = {1,2..H}, η is the effective photo-current conversion ratio, I_h is the normalized received irradiance in the *h-th* hop, x_h is the corresponding modulated signal, and n_h is the additive white Gaussian noise (AWGN) with zero mean and variance $N_0/2$ [12,39].

The irradiance, I_h, fluctuates due to the atmospheric turbulence-induced scintillation effect and the spatial jitter, i.e., the pointing errors effects. Thus, it can be expressed as [12,35,39]:

$$I_h = I_{a,h} I_{p,h}, \tag{2}$$

where $I_{a,h}$ and $I_{p,h}$ represent the irradiance component due to turbulence and pointing errors, respectively. It should be mentioned here that without loss of generality, in (2), the deterministic path loss parameter has been omitted because it is assumed to be normalized to unity [12,15].

2.1. Scintillation Model

The PDF of the MG distribution, as a function of the irradiance $I_{a,h}$ in the *h-th* hop, is given as [19,20,36]:

$$f_{I_{a,h}}(I_{a,h}) = \sum_{i=1}^{N} w_i f_i(I_{a,h}) = \sum_{i=1}^{N} a_i I_{a,h}^{b_i - 1} e^{-\zeta_i I_{a,h}}, I_{a,h} > 0, \tag{3}$$

where $w_i = a_i\Gamma(b_i)\zeta_i^{-b_i}$ with $\sum_{i=1}^{N} w_i = 1$, N is the number of the summation terms, $f_i(x) = \frac{\zeta_i^{b_i} x^{b_i-1}\exp(-\zeta_i x)}{\Gamma(b_i)}$ is the PDF of a Gamma distribution [19,20], a_i, b_i, ζ_i are the parameters of the *i-th* Gamma component [20], and $\Gamma(.)$ is the Gamma function [19,20,34]. Additionally, the cumulative distribution function (CDF) of MG is given as [19,20]:

$$F_{I_{a,h}}(I_{a,h}) = \sum_{i=1}^{N} a_i\zeta_i^{-b_i}\gamma(b_i, \zeta_i I_{a,h}), \tag{4}$$

where $\gamma(\cdot,\cdot)$ is the lower incomplete Gamma function. Very recently, and aiming to accomplish the derivation of simpler expressions for metrics as bit-error-rate, some models which describe the turbulence-induced fading have been published in the literature, but these works use infinite series expansions for the PDFs [21,22]. Thus, an infinite number of summations is required in order to ensure that the integral over the entire space is equal to one. In our work, we use a model which keeps the PDF property for any finite number of terms, as the integral over the entire space is always equal to one. The reliability of the MG model for the approximation of various statistical distributions depends on the number of summation terms, N [19]. By selecting the appropriate value for N, a minimum value for Kull back-Leibler (KL) divergence between a statistical distribution and its approximation obtained using MG model can be achieved in order to be below a given threshold. The D_{KL} divergence is estimated as [19]:

$$D_{KL} = \int_0^{\infty} f_{I_{a,h}}(I_{a,h}) \ln \frac{f_{I_{a,h}}(I_{a,h})}{\hat{f}_{I_{a,h}}(I_{a,h})} dI_{a,h}, \tag{5}$$

where $f_{I_{a,h}}(I_{a,h})$ is the exact PDF of a specific distribution model, while $\hat{f}_{I_{a,h}}(I_{a,h})$ is the approximated PDF obtained using MG. The approximation can be as accurate, as we need only by increasing the number of sum terms. As shown in detail in [19], for all cases, the KL divergence is estimated below 10^{-3} for $N \geq 10$, and therefore, it can be ensured that the MG distribution is an accurate approximate expression with much lower complexity of mathematical expressions compared to the original distribution models. Generally, the number of terms depends on the parameter values characterizing each PDF for each specific distribution model, i.e., parameters α and β for the gamma-gamma distribution [19]. Additionally, in the case where these parameters vary over time, a re-estimation of N is necessary in order to achieve convergence. This task could be achieved using an adaptive algorithm. However, based on the analysis of [19], the use of a large value for N, e.g., about N = 20, usually implies sufficient convergence.

2.2. Scintillation Model through the MG Distribution

In contrast to [24], where the MG model was used for the approximation of the Málaga distribution, here we emulate NE and GG statistical distributions. Thus, by approximating these two models, MG PDF can be used for the representation of a scintillation effect over the whole intensity range, i.e., GG approximation for weak to strong and NE approximation for strong or saturated.

The PDF of the NE distribution, as a function of the normalized irradiance received at the *h-th* hop, is given as [14]:

$$f_{I_{a,h}}(I_{a,h}) = \exp(-I_{a,h}), \tag{6}$$

Here, on the basis of [19,20,34], for the extraction of the parameters for MG distribution, we match the two PDFs, i.e., (3), (24); the resulting parameters which are obtained, in order to approximate the NE distribution, are as follows [36]:

$$a_i = \theta_i\left[\sum_{j=1}^{N} \theta_j\Gamma(b_j)\zeta_j^{-b_j}\right]^{-1}, \quad b_i = 1, \quad \zeta_i = 1, \quad \theta_i = 1, \tag{7}$$

Furthermore, the PDF of the GG distribution as a function of the normalized irradiance at the *h-th* hop is given as [19]:

$$f_{I_{a,h}}(I_{a,h}) = \frac{2(\alpha_h\beta_h)^{\frac{\alpha_h+\beta_h}{2}}}{\Gamma(\alpha_h)\Gamma(\beta_h)} I_{a,h}^{\frac{\alpha_h+\beta_h}{2}-1} K_{\alpha_h-\beta_h}\left(2\sqrt{\alpha_h\beta_h I_{a,h}}\right), \tag{8}$$

where $K_v(\cdot)$ is the v-*th*-order modified Bessel function of the second kind [19], (Equation 8.432.1 of [40]), and α, β are the effective number of small-scale and large scale eddies of the scattering environment, respectively [25]; the latter can be expressed through the MG distribution with parameters [19]:

$$a_i = \frac{\theta_i}{\sum_{j=1}^{N} \theta_j \Gamma(b_j)\zeta_j^{-b_j}}, \; b_i = \alpha_h, \zeta_i = \frac{\alpha_h\beta_h}{t_i}, \; \theta_i = \frac{(\alpha_h\beta_h)^{\alpha_h} w_i t_i^{-\alpha_h+\beta_h-1}}{\Gamma(\alpha_h)\Gamma(\beta_h)}, \tag{9}$$

where w_i and t_i are the weight factors and the abscissas, respectively [19].

2.3. NZB-PE Model

Another significant performance mitigation factor in FSO systems is the misalignment between the transmitter and the receiver, known as the pointing errors effect [12]. This effect results in intensity fluctuations in the received signal, which degrade the performance of FSO systems [12].The Beckmann's model is a statistical model which accurately describes the pointing errors effect and which takes into account the effect of the beam width, detector size, the different jitters for the elevation and the horizontal displacement and the nonzero boresight error [15,41].The Beckmann's model can be accurately approximated through the modified Rayleigh distribution as [12,15,33]:

$$f_{R,h}(R_h) = \frac{R_h}{\sigma^2_{\text{mod},h}} \exp\left(-\frac{R_h^2}{2\sigma^2_{\text{mod},h}}\right), R_h \geq 0, \tag{10}$$

with [12,33]:

$$\sigma^2_{\text{mod},h} = \left(\frac{3\mu^2_{x,h}\sigma^4_{x,h} + 3\mu^2_{y,h}\sigma^4_{y,h} + \sigma^6_{x,h} + \sigma^6_{y,h}}{2}\right)^{1/3} \tag{11}$$

where R_h is the radial displacement in the *h-th* hop, and is expressed as $\left|\vec{R_h}\right| = \sqrt{R^2_{x,h} + R^2_{y,h}}$. At the receiver aperture plane, the radial displacement vector is expressed as $\vec{R_h} = [R_{x,h}, R_{y,h}]^T$, where $R_{x,h}$ and $R_{y,h}$ represent the displacements located along the horizontal and elevation axes respectively, at the detector's plane [12,18,33,42]. In contrast to [23,32], where independent identical zero mean Gaussian distributions for both horizontal and elevation displacement are considered, i.e., the radial displacement R_h at the receiver is modeled through a Rayleigh distribution, we consider a nonzero boresight error, which models $R_{x,h}$ and $R_{y,h}$ as nonzero mean Gaussian distributed random variables with non-identical jitters, with $R_{x,h} = N(\mu_{x,h}, \sigma_{x,h})$ and $R_{y,h} = N(\mu_{y,h}, \sigma_{y,h})$, where $\sigma_{x,h}$ and $\sigma_{y,h}$ are the standard deviation, i.e., the different jitters of the horizontal and elevation displacement respectively, and $\mu_{x,h}$, $\mu_{y,h}$ are the different boresight errors in each axis of the receiver plane $s_h^2 = \mu^2_{x,h} + \mu^2_{y,h}$ [33].

Thus, the PDF as function of $I_{p,m}$ for the NZB-PE effect is approximated as [12,33,36]:

$$f_{I_{p,h}}(I_{p,h}) = \frac{\psi_h^2}{\left(A_{0,h}g_h\right)^{\psi_h^2}} I_{p,h}^{\psi_h^2-1} \text{for } 0 \leq I_{p,h} \leq A_{0,h}g_h, \tag{12}$$

where $\psi_h = w_{z,eq,h}/(2\sigma_{\mathrm{mod},h})$, $\psi_{x,h} = w_{z,eq,h}/(2\sigma_{x,h})$, $\psi_{y,h} = w_{z,eq,h}/(2\sigma_{y,h})$, and [12,33],

$$g_h = \exp\left(\frac{1}{\psi_h^2} - \frac{1}{2\psi_{x,h}^2} - \frac{1}{2\psi_{y,h}^2} - \frac{\mu_{x,h}^2}{2\sigma_{x,h}^2\psi_{x,h}^2} - \frac{\mu_{y,h}^2}{2\sigma_{y,h}^2\psi_{y,h}^2}\right) \tag{13}$$

Additionally,$w_{z,eq,h}$ is the equivalent beam radius in the *h-th* hop, which is given as $w_{z,eq,h}^2 = \sqrt{\pi}erf(u_h)w_{z,h}^2/\left[2u_h\exp\left(-u_h^2\right)\right]$, where $u_h = \sqrt{\pi}r_{a,h}/\sqrt{2}w_{z,h}$, with $r_{a,h}$ being the radius of the circular detection aperture, $w_{z,h}$ the waist of the Gaussian's beam, spatial intensity profile, and $erf(.)$ representing the error function. Generally speaking, the performance of the system can be significantly increased if detection is achieved near the center of the pulse. It should be mentioned here that the considered NZB-PE model is accurate enough when the normalized beam width $w_{z,h}/r_h > 6$, which is satisfied for typical terrestrial FSO systems, where r_h is the radius of the receiver aperture [12,33]. Furthermore, $A_{0,h}$ is the fraction of the collected power at $r_{a,h} = 0$ [15,32,33], with $A_{0,h} = [erf(u_h)]^2$. Here, it should be mentioned that the impact of the pointing errors effect becomes less important as the value of ψ_h increases; thus, for large values of ψ_h, this damaging effect can be considered negligible. Note that the PDF of the nonzero boresight pointing errors model can be easily reduced to this with zero boresight [12,15,32]. Considering independent identical zero mean Gaussian distributions for both elevation and horizontal displacement, the PDF for the zero boresight scenario is defined as in (12), with $g_h = 1$, $\mu_{x,h}^2 = 0$, $\mu_{y,h}^2 = 0$, $\sigma_{x,h}^2 = \sigma_{y,h}^2 = \sigma_{s,h}^2$ [12].

2.4. The Composite Irradiance Model

The composite PDF of irradiance, I_h, which arrives at the receiver side, by including both scintillation and pointing errors effects influence, (2), is estimated as [12,19,42]:

$$f_{I_h}(I_h) = \int f_{I_h|I_{a,h}}(I_h|I_{a,h})f_{I_{a,h}}(I_{a,h})dI_{a,h} \tag{14}$$

where $f_{I_h|I_{a,h}}(I_h|I_{a,h}) = \frac{1}{I_{a,h}}f_{I_{p,h}}\left(\frac{I_h}{I_{a,h}}\right)$ represents the conditional probability of $I_{a,h}$. Thus, from (12), we get [12,19]:

$$f_{I_h|I_{a,h}}(I_h|I_{a,h}) = \frac{\psi_h^2}{(A_{0,h}g_h)^{\psi_h^2}}\left(\frac{I_h^{\psi_h^2-1}}{I_{a,h}^{\psi_h^2}}\right), \text{ with } 0 \le I_h \le (A_{0,h}g_h)I_{a,h}, \tag{15}$$

Next, by substituting (3), (15) into (14), the following integral is obtained:

$$f_{I_h}(I_h) = \frac{\psi_h^2}{(A_{0,h}g_h)^{\psi_h^2}}I_h^{\psi_h^2-1}\sum_{i=1}^{N}a_i\int_{I_h/(A_{0,h}g_h)}^{\infty}I_{a,h}^{b_i-1-\psi_h^2}\exp\left(-\zeta_i I_{a,h}\right)dI_{a,h} \tag{16}$$

and the analytical outcome for the composite PDF is derived based on [19] and by using (Equation 3.381.3 of [40]), as:

$$f_{I_h}(I_h) = \frac{\psi_h^2}{(A_{0,h}g_h)^{\psi_h^2}}I_h^{\psi_h^2-1}\sum_{i=1}^{N}a_i\zeta_i^{\psi_h^2-b_i}\Gamma\left(b_i-\psi_h^2, \frac{\zeta_i}{A_{0,h}g_h}I_h\right), \text{ for } I_h > 0, \tag{17}$$

with a_i, b_i and ζ_i being the parameters of the MG distribution, as in (3). Thus, (17) can be used for the emulation of all the statistical models under consideration by changing the values of these parameters. Moreover, $\Gamma(\cdot,\cdot)$ is the upper incomplete Gamma function defined in (Equation 8.350.2

of [40]). Furthermore, the CDF for I_h is obtained from (Equation 8.356.3 of [40]) and (Equation 06.06.21.0002.01 of [43]) as [19]:

$$F_{I_h}(I_h) = \sum_{i=1}^{N} a_i \zeta_i^{-b_i} \left[\left(\frac{\zeta_i I_h}{A_{0,h} g_h} \right)^{\psi_h^2} \Gamma\left(b_i - \psi_h^2, \frac{\zeta_i I_h}{A_{0,h} g_h} \right) + \gamma\left(b_i, \frac{\zeta_i I_h}{A_{0,h} g_h} \right) \right], \tag{18}$$

Next, the instantaneous electrical SNR and expected electrical SNR at the receiver in the *h-th* hop can be defined as $\gamma_h = (\eta I_h)^2 / \sigma_n^2$ and $\mu_h = (\eta E[I_h])^2 / \sigma_n^2$ for IM/DD detection, respectively [15,24,44,45], while the expected value of irradiance, i.e., $E[I_h]$, can be estimated through the general integral for the *k-th* moment estimation, $E\left[I_h^k\right] = \int_0^\infty I_h^k f_{I_h}(I_h) dI_h$, by assuming $k = 1$, as follows [19]:

$$E\left[I_h\right] = \frac{\psi_h^2 A_{0,h} g_h}{1 + \psi_h^2} \sum_{i=1}^{N} a_i \zeta_i^{-(1+b_i)} \Gamma(1 + b_i), \tag{19}$$

Then, by using the expression for the SNR definition with a random variable (RV) transformation [24], the PDF of (17) is transformed to the following PDF as a function of γ_h:

$$\begin{aligned} f_{\gamma_h}(\gamma_h) &= \frac{\psi_h^2}{2(A_{0,h} g_h)\psi_h^2} \frac{E[I_h]^{\psi_h^2}}{\mu_h^{(\psi_h^2/2)}} \gamma_h^{(\psi_h^2/2)-1} \\ &\times \sum_{i=1}^{N} a_i \zeta_i^{\psi_h^2 - b_i} \Gamma\left(b_i - \psi_h^2, \frac{\zeta_i E[I_h]}{A_{0,h} g_h} \sqrt{\frac{\gamma_h}{\mu_h}} \right), \mu_h > 0 \end{aligned} \tag{20}$$

while the corresponding CDF is obtained by substituting the expression (20) into the integral as [24]:

$$\begin{aligned} F_{\gamma_h}(\gamma_h) = \int_0^{\gamma_h} f_{\gamma_h(\gamma_h)} d\gamma_h &= \int_0^{\gamma_h} \frac{\psi_h^2}{2(A_{0,h} g_h)\psi_h^2} \frac{E[I_h]^{\psi_h^2}}{\mu_h^{(\psi_h^2/2)}} \gamma_h^{(\psi_h^2/2)-1} \times \\ &\times \sum_{i=1}^{N} a_i \zeta_i^{\psi_h^2 - b_i} \Gamma\left(b_i - \psi_h^2, \frac{\zeta_i E[I_h]}{A_{0,h} g_h} \sqrt{\frac{\gamma_h}{\mu_h}} \right) d\gamma_h. \end{aligned} \tag{21}$$

Hence, the closed form mathematical expression of the corresponding CDF can be given as [24]:

$$\begin{aligned} F_{\gamma_h}(\gamma_h) &= \sum_{i=1}^{N} a_i \zeta_i^{-b_i} \left[\left(\frac{\zeta_i E[I_h]}{A_{0,h} g_h} \sqrt{\frac{\gamma_h}{\mu_h}} \right)^{\psi_h^2} \times \right. \\ &\left. \times \Gamma\left(b_i - \psi_h^2, \frac{\zeta_i E[I_h]}{A_{0,h} g_h} \sqrt{\frac{\gamma_h}{\mu_h}} \right) + \gamma\left(b_i, \frac{\zeta_i E[I_h]}{A_{0,h} g_h} \sqrt{\frac{\gamma_h}{\mu_h}} \right) \right] \end{aligned} \tag{22}$$

3. Performance of the Link

In this section, novel analytical expressions for the performance estimation of a serial DF relayed FSO system which operates under the combined impact of nonzero boresight pointing errors and an MG-modeled scintillation effect are derived for first time. Here, we should mention that, in contrast to [24], where the performance of a traditional FSO system which operates by using a single point-to-point link with a DBPSK modulation format was studied, in our work, we investigate one more significant issue which concerns the way in which the effective radius of the FSO links can be extended by using DF relay nodes, and we establish the most typical and realistic modulation formats for the FSO links, i.e., OOK and PPM, while amore generalized model which takes into account a nonzero boresight impact, has been adopted for the pointing errors impact.

3.1. OP of the Composite FSO System

The probability of outage represents a significant metric for the system's reliability, since it expresses the probability that the instantaneous SNR falls below a critical threshold, $\gamma_{th,h}$, which

corresponds to the sensitivity limit of each receiver [44]. Thus, using the above derived CDF, (22), the OP of the *h-th* hop is given as [15,38,44]:

$$P_{out,h} = \Pr\left(\gamma_h \le \gamma_{th,h}\right) = F_{\gamma_h}(\gamma_{th,h}) = \sum_{i=1}^{N} a_i \zeta_i^{-b_i} \left[\left(\frac{\zeta_i E[I_h]}{A_{0,h} g_h} \sqrt{\frac{\gamma_{th,h}}{\mu_h}} \right)^{\psi_h^2} \times \Gamma\left(b_i - \psi_h^2, \frac{\zeta_i E[I_h]}{A_{0,h} g_h} \sqrt{\frac{\gamma_{th,h}}{\mu_h}} \right) + \gamma\left(b_i, \frac{\zeta_i E[I_h]}{A_{0,h} g_h} \sqrt{\frac{\gamma_{th,h}}{\mu_h}} \right) \right] \tag{23}$$

Subsequently, the closed form mathematical expression for the total OP of the system with H serial DF hops and a wide range of turbulence conditions, along with pointing errors impact with nonzero bore sight, are given as [15,35,38]:

$$P_{out} = 1 - \prod_{h=1}^{H} \left[1 - P_{out,h} \right], \tag{24}$$

and by substituting (23) into (24), we finally get the OP of the whole DF relayed FSO system:

$$P_{out} = 1 - \prod_{h=1}^{H} \left\{ 1 - \sum_{i=1}^{N} a_i \zeta_i^{-b_i} \times \left[\left(\frac{\zeta_i E[I_h]}{A_{0,h} g_h} \left(\frac{\gamma_{th,h}}{\mu_h} \right)^{1/2} \right)^{\psi_h^2} \times \Gamma\left(b_i - \psi_h^2, \frac{\zeta_i E[I_h]}{A_{0,h} g_h} \left(\frac{\gamma_{th,h}}{\mu_h} \right)^{1/2} \right) + \gamma\left(b_i, \frac{\zeta_i E[I_h]}{A_{0,h} g_h} \left(\frac{\gamma_{th,h}}{\mu_h} \right)^{1/2} \right) \right] \right\} \tag{25}$$

3.2. ABER of the Composite FSO System

The Bit Error Rate (BER) is one of the most well-known and crucial metrics for the performance of communication systems [12]. However, the BER is estimated through the instantaneous electrical SNR at the receiver, which fluctuates; thus, the BER cannot remain constant. Hence, the estimation of the average BER is more useful for the evaluation of the performance of such systems in practice [12]. Motivated by the latter notion, in this section, we investigate the ABER of a serial DF-relayed FSO system with OOK and L-PPM schemes.

First, we consider OOK modulation for the FSO system. Thus, the BER of the *h-th* hop is given as [16]:

$$P_{b,h}^{OOK}(I_h) = Q\left(\sqrt{\frac{(\eta_h I_h)^2}{2N_0}} \right) \tag{26}$$

By integrating the BER expression over I_h, the ABER can be written as [12,16]:

$$P_{b,AV,h}(I_h) = \int_0^{\infty} P_e(I_h) f_{I_h}(I_h) dI_h. \tag{27}$$

By substituting (17), (26) into (27), along with the approximation of [46] for the Q-function, i.e., $Q(x) \approx \left(e^{-x^2/2} + 3e^{-2x^2/3} \right)/12$, and the transformation of (Equation 2.10.3.9 of [47]), the closed form mathematical expression for the ABER of the *h-th* hop for the OOK case is obtained as:

$$P_{b,AV,h}^{OOK} \approx \frac{\psi_h^2}{(A_{0,h} g_h)^{\psi_h^2}} \sum_{i=1}^{N} \left\{ a_i \zeta_i^{\psi_h^2 - b_i} \left[P_1 + P_2 + P_3 + P_4 \right] \right\} \tag{28}$$

where

$$\begin{aligned} P_1 &= -\mathrm{X}(0)\mathrm{Z}(4,0)\Gamma(b_i/2)\Psi_1 \\ P_2 &= \mathrm{X}(1)\mathrm{Z}(4,1)\Gamma((b_i+1)/2)\Psi_2(1) + \Omega(4) \\ P_3 &= -\mathrm{X}(0)\mathrm{Z}(3,0)\Gamma(b_i/2)\Psi_1(3/4) \\ P_4 &= \mathrm{X}(1)\mathrm{Z}(3,1)\Gamma((b_i+1)/2)\Psi_2(3/4) + \Omega(3) \end{aligned}$$

with

$$\mathrm{X}(y) = \frac{\zeta_i^{b_i-\psi_h^2+y}}{2(b_i-\psi_h^2+y)(A_{0,h}g_h)^{b_i-\psi_h^2+y}}$$
$$\Omega(z) = \frac{\Gamma(b_i-\psi_h^2)\Gamma(\psi_h^2/2)}{2(\mu_h/zE^2[I_h])^{\psi_h^2/2}}$$
$$\mathrm{Z}(w,t) = \left(\frac{\mu_h}{wE^2[I_h]}\right)^{-(b_i+t)/2}$$
$$\Psi_1(x) = {}_2F_2\left(\frac{b_i-\psi_h^2}{2}, \frac{b_i}{2}; \frac{1}{2}, \frac{b_i-\psi_h^2}{2}+1; \frac{x\zeta_i^2E^2[I_h]}{(A_{0,h}g_h)^2\mu_h}\right)$$
$$\Psi_2(x) = {}_2F_2\left(\frac{b_i-\psi_h^2+1}{2}, \frac{b_i+1}{2}; \frac{3}{2}, \frac{b_i-\psi_h^2+3}{2}; \frac{x\zeta_i^2E^2[I_h]}{(A_{0,h}g_h)^2\mu_h}\right),$$

where ${}_2F_2(\cdot,\cdot;,\cdot;\cdot)$ is the generalized hypergeometric series (Equation 9.14.1 of [40]).

Next, for the *L*-PPM scheme, the BER of the *h-th* hop is given as [16]:

$$P_{b,h}^{L-PPM} = \frac{L}{2}Q\left(\sqrt{\frac{L(\eta_h I_h)^2\log_2(L)}{4N_0}}\right). \tag{29}$$

Following the same methodology as that of the OOK case, we substitute (29) into (27). Thus, the ABER of the *h-th* hop for the *L*-PPM scheme is obtained through the following expression, as:

$$P_{b,AV,h}^{L-PPM} \approx \frac{\psi_h^2 L}{24(A_{0,h}g_h)^{\psi_h^2}}\sum_{i=1}^{N}\left\{a_i\zeta_i^{\psi_h^2-b_i}[P_A+P_B+P_C+P_D]\right\} \tag{30}$$

where

$$P_A = -\mathrm{X}(0)\Phi(8,0)\Gamma(b_i/2)\Psi_1(2)$$
$$P_B = \mathrm{X}(1)\Phi(8,1)\Gamma((b_i+1)/2)\Psi_2(2)+\mathrm{T}(8)$$
$$P_C = -\tfrac{3}{2}\mathrm{X}(0)\Phi(6,0)\Gamma(b_i/2)\Psi_1(3/2)$$
$$P_D = \tfrac{3}{2}\mathrm{X}(1)\Phi(6,1)\Gamma((b_i+1)/2)\Psi_2(3/2)+3\mathrm{T}(6)$$

with

$$\mathrm{T}(z) = \frac{\Gamma(b_i-\psi_h^2)\Gamma(\psi_h^2/2)}{2(\mu_h L\log_2(L)/zE^2[I_h])^{\psi_h^2/2}}$$
$$\Phi(w,t) = \left(\frac{\mu_h L\log_2(L)}{wE^2[I_h]}\right)^{-(b_i+t)/2}$$

The total average BER of the whole DF relayed FSO system, is given as [48–50]:

$$P_{b,AV} = \sum_{h=1}^{H}\left\{P_{b,AV,h}\prod_{k=h+1}^{H}\left[1-2P_{b,AV,h}\right]\right\} \tag{31}$$

where $P_{b,AV,h}$ could be either the ABER of OOK, (28), or the ABER of *L*-PPM, (30). Thus, the average BER of the whole DF relayed FSO system with OOK modulation and NZB-PE over MG scintillation is given as:

$$P_{b,AV}^{OOK} = \sum_{h=1}^{H}\left\{\left[\frac{\psi_h^2}{(A_{0,h}g)^{\psi_h^2}}\sum_{i=1}^{N}a_i\zeta_i^{\psi_h^2-b_i}[P_1+P_2+P_3+P_4]\right]\times \right.$$
$$\left.\times\prod_{k=h+1}^{H}\left[1-2\left[\frac{\psi_h^2}{(A_{0,h}g)^{\psi_h^2}}\sum_{i=1}^{N}a_i\zeta_i^{\psi_h^2-b_i}[P_1+P_2+P_3+P_4]\right]\right]\right\}, \tag{32}$$

while the corresponding average BER expression for the *L*-PPM scheme is given as:

$$P_{b,AV}^{L-PPM} = \sum_{h=1}^{H} \left\{ \left[\frac{\psi_h^2 L}{24(A_{0,h}g)^{\psi^2}} \sum_{i=1}^{N} a_i \zeta_i^{\psi_h^2 - b_i} [P_A + P_B + P_C + P_D] \right] \times \right.$$
$$\left. \times \prod_{k=h+1}^{H} \left[1 - 2 \left[\frac{\psi_h^2 L}{24(A_{0,h}g)^{\psi_h^2}} \sum_{i=1}^{N} a_i \zeta_i^{\psi_h^2 - b_i} [P_A + P_B + P_C + P_D] \right] \right] \right\} \quad (33)$$

4. Numerical Results

In this section, we present the performance results using the estimation of OP and the average BER, through the above derived expressions, (25), (32) and (33), along with the parameter values from expressions (7) and (9). More analytically, expressions (25), (32) and (33) estimate the performance of NE case by the substitution of (7), while for the GG case, this is achieved by the substitution of (9). Hence, only by selecting the appropriate set for the MG model parameters', we can estimate the combined impact of NZB-PE, along with the whole intensity range of the scintillation effect.For the numerical results, we consider $w_{z,h}/r_h = 7$, based on [12,33]. More precisely, by assuming a receiver aperture radius of $r_h = 0.05\ m$, the waist of the Gaussian beam spatial intensity profile becomes $w_{z,h} = 0.35$. The standard deviations and the means of the horizontal and the elevation displacement take the values $\sigma_{x,h} = 0.1$, $\sigma_{y,h} = 0.05$, $\mu_{x,h} = 0.05$, and $\mu_{y,h} = 0.1$, respectively. Hence, $u_h \approx 0.18$ and, $w_{z,eq,h}^2 \approx 0.125$, while $\psi_{x,h} \approx 1.77$ and $\psi_{y,h} \approx 3.54$. For the case of NE distribution, we assume that $N = 1$, while for the GG case, N = 10 is considered in order to ensure that the MG distribution is an accurate approximation of the GG distribution [19]. Moreover, without loss of generality and for the sake of simplicity, for the GG parameters, we use the values $\alpha_1 = \alpha_h = \alpha$, and $\beta_1 = \beta_h = \beta$ for all the H different hops. It should be noted here that any valid set of α and β can be used to achieve the desired intensity of the scintillation effect. Furthermore, we make the same assumptions for the PE parameters, i.e., $\psi_1 = \psi_h = \psi$, $A_{0,1} = A_{0,h} = A_0$, $g_1 = g_h = g$, and finally, for the average electrical SNR, $\mu_1 = \mu_h = \mu$. The parameter values used here are shown in Table 1.

Table 1. Values of turbulence and pointing errors parameters.

Distributions	α	β	ψ	A_0	g
NE	-	-	2.52	0.04	0.79
GG	2	5	1.3	0.04	1.21

All the figures given below demonstrate the numerical results of our work which were obtained from the above derived closed form mathematical expressions (25), (32) and (33), which are the main analytical outcomes of this manuscript. More precisely, Figure 1, demonstrates the OP results, obtained from the above derived Equation (25), versus the normalized outage threshold $\mu/\gamma_{th,m}$ for the case where the MG model approximates NE or GG distribution, while Figures 2–4, demonstrate the outcomes of the above derived Equations (32) and (33) for the average BER versus electrical SNR for the same approximations, with the OOK, 4-PPM and 16-PPM schemes, respectively.

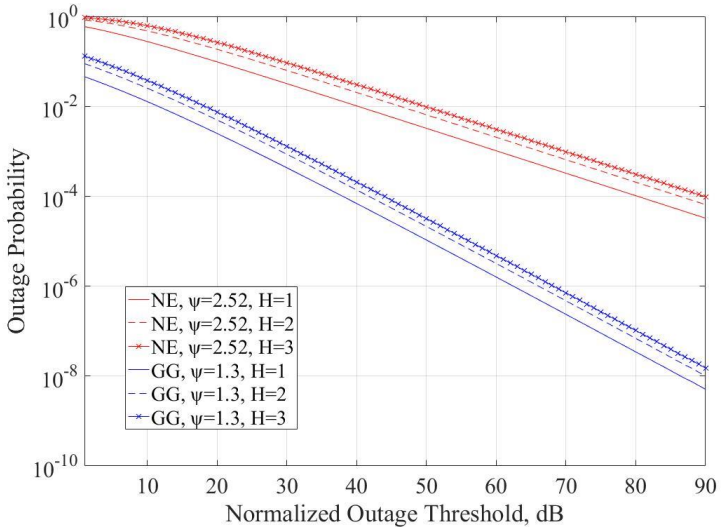

Figure 1. OP versus the normalized outage threshold.

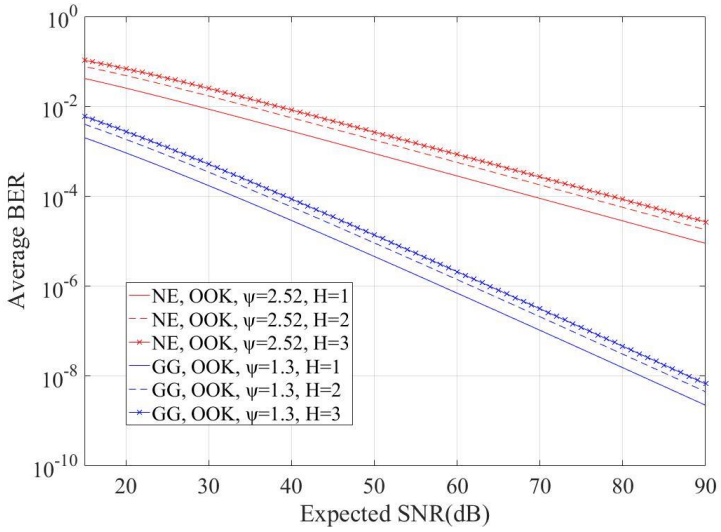

Figure 2. ABER ofOOK scheme versus the expected SNR.

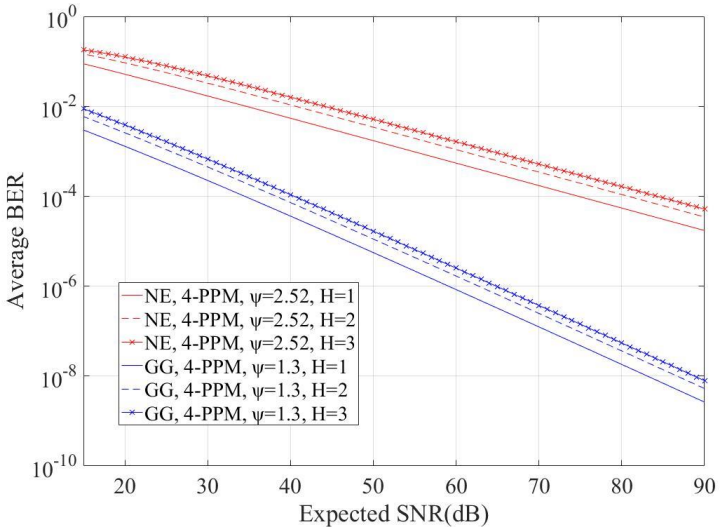

Figure 3. ABER of 4-PPM scheme versus the expected SNR.

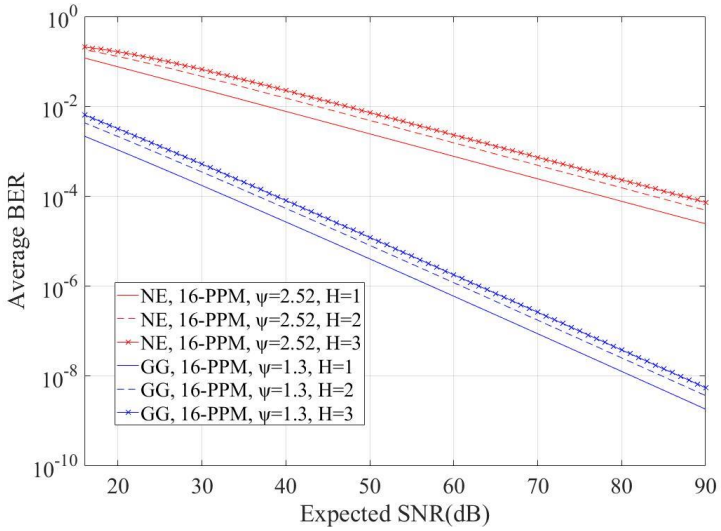

Figure 4. ABER of16-PPM scheme versus the expected SNR.

As shown from the numerical results, even though the FSO system operates over a composite channel with a pointing errors effect with nonzero boresight, along with a wide range of turbulence conditions—i.e., from weak to strong by using the approximation of GG, or saturated by using the approximation of NE—, the serial DF relayed link, with more than one hop, e.g., $H = 2$ or 3, can maintain its performance and reliability over much longer propagation distances, i.e., $2D$ or $3D$, respectively, compared with the classical scenario with only one hop, i.e., $H = 1$, where the propagation distance being D. Additionally, the numerical results demonstrate that if the main demand of the system coincides with maximal reliability, the OOK slightly outperforms the other modulation schemes for the NE case, while in the GG case, the reliability is almost the same for all modulation schemes. On the other hand, if a high data rate is the purpose, the use of 16-PPM is preferable.

5. Conclusions

In this work, a serial DF relayed FSO system with OOK or L-PPM modulation scheme, which operates under the combined impact of atmospheric turbulence and nonzero boresight pointing errors, has been studied. Additionally, the scintillation effect has been approximated through the MG distribution for the simplification of mathematical expressions used for such composite channels with pointing errors, along with atmospheric turbulence effect. Furthermore, we derived general closed form analytical expressions for the OP and the average BER of a serial DF relayed FSO system, which only by selecting the appropriate values for the MG model, can be used for the evaluation of composite channels with pointing errors along with a wide range of turbulence conditions i.e. from week to strong or saturated.

Author Contributions: Conceptualization, N.A.A. and H.E.N.; methodology, N.A.A. and H.E.N.; software, N.A.A.; validation, N.A.A., H.E.N. and H.K.; formal analysis, N.A.A. and H.E.N.; investigation, N.A.A., H.E.N., H.K., S.S.M. and G.S.T.; resources, N.A.A., H.E.N., H.K., S.S.M. and G.S.T.; writing—original draft preparation, N.A.A.; writing—review and editing, H.E.N., S.S.M., G.S.T.; supervision, H.E.N.; project administration, G.S.T.; funding acquisition, H.E.N., G.S.T.

Funding: H.E.N. and G.S.T. acknowledges the funding from the European Union's Horizon 2020 research and innovation program under grant agreement No: 777596. N.A.A. acknowledges that this research is co-financed by Greece and the European Union (European Social Fund- ESF) through the Operational Program "Human Resources Development, Education and Lifelong Learning" in the context of the project "Strengthening Human Resources Research Potential via Doctorate Research" (MIS-5000432), implemented by the State Scholarships Foundation (IKϒ).

Conflicts of Interest: The authors declare no conflict of interest.

References

1. Ghassemlooy, Z.; Popoola, W.O. Terrestrial Free-Space Optical Communications. In *Mobile and Wireless Communications Network Layer and Circuit Level Design*; InTech: London, UK, 2010. [CrossRef]
2. Majumdar, A.K. Fundamentals of Free-Space Optical (FSO) Communication System. In *Advanced Free Space Optics (FSO): A Systems Approach*; Springer Series in Optical Sciences: New York, NY, USA, 2015; pp. 1–20.
3. Ghassemlooy, Z.; Arnon, S.; Uysal, M.; Xu, Z.; Cheng, J. Emerging Optical Wireless Communications-Advances and Challenges. *IEEE J. Sel. Areas Commun.* **2015**, *33*, 1738–1749. [CrossRef]
4. Khalighi, M.A.; Uysal, M. Survey on Free Space Optical Communication: A Communication Theory Perspective. *IEEE Commun. Surv. Tutor.* **2014**, *16*, 2231–2258. [CrossRef]
5. Djordjevic, G.; Petkovic, M.; Cvetkovic, A.; Karagiannidis, G. Mixed RF/FSO Relaying with Outdated Channel State Information. *IEEE J. Sel. Areas Commun.* **2015**, *33*, 1935–1948. [CrossRef]
6. Djordjevic, G.T.; Petkovic, M.I.; Spasic, M.; Antic, D.S. Outage Capacity of FSO Link with Pointing Errors and Link Blockage. *Opt. Express* **2016**, *24*, 219–230. [CrossRef]
7. Tsonev, D.; Sinanovic, S.; Haas, H. Complete Modeling of Nonlinear Distortion in OFDM-Based Optical Wireless Communication. *J. Light. Technol.* **2013**, *31*, 3064–3076. [CrossRef]
8. Dimitrov, S.; Sinanovic, S.; Haas, H. Clipping Noise in OFDM-Based Optical Wireless Communication Systems. *IEEE Trans. Commun.* **2012**, *60*, 1072–1081. [CrossRef]
9. Leitgeb, E.; Gebhart, M.; Birnbacher, U. Optical Networks, Last Mile Access and Applications. *J. Opt. Fiber Commun. Rep.* **2005**, *2*, 56–85. [CrossRef]
10. Gappmair, W.; Hranilovic, S.; Leitgeb, E. OOK Performance for Terrestrial FSO Links in Turbulent Atmosphere with Pointing Errors Modeled by Hoyt Distributions. *IEEE Commun. Lett.* **2011**, *15*, 875–877. [CrossRef]
11. Epple, B. Simplified Channel Model for Simulation of Free-Space Optical Communications. *J. Opt. Commun. Netw.* **2010**, *2*, 293. [CrossRef]
12. Varotsos, G.K.; Nistazakis, H.E.; Petkovic, M.I.; Djordjevic, G.T.; Tombras, G.S. SIMO Optical Wireless Links with Nonzero Boresight Pointing Errors over M Modeled Turbulence Channels. *Opt. Commun.* **2017**, *403*, 391–400. [CrossRef]
13. Andrews, L.C.; Phillips, R.L. Classical Theory for Propagation Through Random Media. In *Laser Beam Propagation through Random Media*, 2nd ed.; SPIE—The International Society for Optical Engineering: Washington, DC, USA, 2005; pp. 135–177.
14. Nistazakis, H.E. A Time-Diversity Scheme for Wireless Optical Links over Exponentially Modeled Turbulence Channels. *Optik* **2013**, *124*, 1386–1391. [CrossRef]
15. Varotsos, G.; Nistazakis, H.E.; Stassinakis, A.N.; Volos, C.K.; Christofilakis, V.; Tombras, G.S. Mixed Topology of DF Relayed Terrestrial Optical Wireless Links with Generalized Pointing Errors over Turbulence Channels. *Technologies* **2018**, *6*, 121. [CrossRef]
16. Ninos, M.P.; Nistazakis, H.E.; Tombras, G.S. On the BER Performance of FSO Links with Multiple Receivers and Spatial Jitter over Gamma-Gamma or Exponential Turbulence Channels. *Optik* **2017**, *138*, 269–279. [CrossRef]
17. Jurado-Navas, A.; Garrido-Balsells, J.M.; Paris, J.F.; Castillo-Vazquez, M.; Puerta-Notario, A. Further Insights onMálaga Distribution for Atmospheric Optical Communications. In Proceedings of the 2012 International Workshop on Optical Wireless Communications (IWOW), Pisa, Italy, 22 October 2012; pp. 5–7. [CrossRef]
18. Ninos, M.P.; Nistazakis, H.E.; Sandalidis, H.; Tombras, G.S. CDMA RoFSO Links with Nonzero Boresight Pointing Errors over M Turbulence Channels. *IEEE Photonics J.* **2018**, *10*, 1–12. [CrossRef]
19. Sandalidis, H.G.; Chatzidiamantis, N.D.; Karagiannidis, G.K. A Tractable Model for Turbulence- and Misalignment-Induced Fading in Optical Wireless Systems. *IEEE Commun. Lett.* **2016**, *20*, 1904–1907. [CrossRef]
20. Atapattu, S.; Tellambura, C.; Jiang, H. A Mixture Gamma Distribution to Model the SNR of Wireless Channels. *IEEE Trans. Wirel. Commun.* **2011**, *10*, 4193–4203. [CrossRef]
21. Bhatnagar, M.R.; Ghassemlooy, Z. Performance Analysis of Gamma–Gamma Fading FSO MIMO Links With Pointing Errors. *J. Light. Technol.* **2016**, *34*, 2158–2169. [CrossRef]
22. Bhatnagar, M.R. A One Bit Feedback Based Beamforming Scheme for FSO MISO System Over Gamma-Gamma Fading. *IEEE Trans. Commun.* **2015**, *63*, 1306–1318. [CrossRef]

23. Sandalidis, H.G.; Tsiftsis, T.A.; Karagiannidis, G.K. Optical Wireless Communications With Heterodyne Detection Over Turbulence Channels With Pointing Errors. *J. Light. Technol.* **2009**, *27*, 4440–4445. [CrossRef]
24. Sandalidis, H.G.; Chatzidiamantis, N.D.; Ntouni, G.D.; Karagiannidis, G.K. Performance of Free-Space Optical Communications over a Mixture Composite Irradiance Channel. *Electron. Lett.* **2017**, *53*, 260–262. [CrossRef]
25. Gappmair, W.; Nistazakis, H.E. Subcarrier PSK Performance in Terrestrial FSO Links Impaired by Gamma-Gamma Fading, Pointing Errors, and Phase Noise. *J. Light. Technol.* **2017**, *35*, 1624–1632. [CrossRef]
26. Gappmair, W.; Hranilovic, S.; Leitgeb, E. Performance of PPM on Terrestrial FSO Links with Turbulence and Pointing Errors. *IEEE Commun. Lett.* **2010**, *14*, 468–470. [CrossRef]
27. Laourine, A.; Stephenne, A.; Affes, S. Estimating the Ergodic Capacity of Log-Normal Channels. *IEEE Commun. Lett.* **2007**, *11*, 568–570. [CrossRef]
28. Gappmair, W.; Flohberger, M. Error Performance of Coded FSO Links in Turbulent Atmosphere Modeled by Gamma-Gamma Distributions. *IEEE Trans. Wirel. Commun.* **2009**, *8*, 2209–2213. [CrossRef]
29. Al-Habash, M.A. Mathematical Model for the Irradiance Probability Density Function of a Laser Beam Propagating through Turbulent Media. *Opt. Eng.* **2001**, *40*, 1554. [CrossRef]
30. Jurado-Navas, A.; Maria, J.; Francisco, J.; Puerta-Notario, A. A Unifying Statistical Model for Atmospheric Optical Scintillation. In *Numerical Simulations of Physical and Engineering Processes*; InTech: London, UK, 2011. [CrossRef]
31. Arnon, S. Effects of Atmospheric Turbulence and Building Sway on Optical Wireless-Communication Systems. *Opt. Lett.* **2003**, *28*, 129–131. [CrossRef]
32. Farid, A.A.; Hranilovic, S. Outage Capacity Optimization for Free-Space Optical Links with Pointing Errors. *J. Light. Technol.* **2007**, *25*, 1702–1710. [CrossRef]
33. Boluda-Ruiz, R.; García-Zambrana, A.; Castillo-Vázquez, C.; Castillo-Vázquez, B. Novel Approximation of Misalignment Fading Modeled by Beckmann Distribution on Free-Space Optical Links. *Opt. Express* **2016**, *24*, 22635. [CrossRef]
34. Miridakis, N.I.; Tsiftsis, T.A. EGC Reception for FSO Systems under Mixture-Gamma Fading Channels and Pointing Errors. *IEEE Commun. Lett.* **2017**, *21*, 1441–1444. [CrossRef]
35. Prabu, K.; Kumar, D.S. Outage Analysis of Relay-Assisted BPSK-SIM Based FSO Systems over Strong Atmospheric Turbulence with Pointing Errors. *IJCCE* **2014**, *3*, 3–6. [CrossRef]
36. Androutsos, N.A.; Nistazakis, H.E.; Stassinakis, A.N.; Sandalidis, H.G.; Tombras, G.S. Performance of SIMO FSO Links over Mixture Composite Irradiance Channels. *Appl. Sci.* **2019**, *9*, 2072. [CrossRef]
37. Elganimi, Y.T. Performance Comparison between OOK, PPM and PAM Modulation Schemes for Free Space Optical (FSO) Communication Systems: Analytical Study. *Int. J. Comput. Appl.* **2013**, *79*, 22–27. [CrossRef]
38. Feng, M.; Wang, J.; Sheng, M.; Cao, L.; Chen, X.X.M. Outage Performance for Parallel Relay-Assisted Free-Space Optical Communications in Strong Turbulence with Pointing Errors. In Proceedings of the 2011 International Conference on Wireless Communications and Signal Processing (WCSP), Nanjing, China, 9–11 November 2011; pp. 7–11. [CrossRef]
39. Varotsos, G.K.; Nistazakis, H.E.; Volos, C.K.; Tombras, G.S. FSO Links with Diversity Pointing Errors and Temporal Broadening of the Pulses over Weak to Strong Atmospheric Turbulence Channels. *Optik* **2016**, *127*, 3402–3409. [CrossRef]
40. Gradshteyn, I.S.; Ryzhik, I.M. Special Functions. In *Table of Integrals, Series, and Products*, 7th ed.; Jeffrey, A., Zwillinger, D., Eds.; Elsevier (Academic Press): New York, NY, USA, 2008; pp. 859–1046.
41. Boluda-Ruiz, R.; García-Zambrana, A.; Castillo-Vázquez, B.; Castillo-Vázquez, C. Impact of Nonzero Boresight Pointing Error on Ergodic Capacity of MIMO FSO Communication Systems. *Opt. Express* **2016**, *24*, 3513. [CrossRef] [PubMed]
42. Yang, F.; Cheng, J.; Tsiftsis, T.A. Free-Space Optical Communication with Nonzero Boresight Pointing Errors. *IEEE Trans. Commun.* **2014**, *62*, 713–725. [CrossRef]
43. The Wolfarm Functions Site. Available online: http://functions.wolfarm.com (accessed on 10 April 2019).
44. Katsis, A.; Nistazakis, H.E.; Tombras, G.S. Bayesian and Frequentist Estimation of the Performance of Free Space Optical Channels under Weak Turbulence Conditions. *J. Frankl. Inst.* **2009**, *346*, 315–327. [CrossRef]
45. AlQuwaiee, H.; Ansari, I.S.; Alouini, M.-S. On the Performance of Free-Space Optical Communication Systems Over Double Generalized Gamma Channel. *IEEE J. Sel. Areas Commun.* **2015**, *33*, 1829–1840. [CrossRef]

46. Chiani, M.; Dardari, D.; Simon, M.K. New Exponential Bounds and Approximations for the Computation of Error Probability in Fading Channels. *IEEE Trans. Wirel. Commun.* **2003**, *24*, 840–845. [CrossRef]
47. Prudnikov, A.P.; Brychkov, Y.A.; Marichev, O.I. Definite Integrals. In *Integrals and Series: Special Functions*; Gordon and Breach Science Publishers: Glasgow, UK, 1992; Volume 2, pp. 55–612.
48. Sheng, M.; Jiang, P.; Hu, Q.; Su, Q.; Xie, X. End-to-End Average BER Analysis for Multihop Free-Space Optical Communications with Pointing Errors. *J. Opt.* **2013**, *15*. [CrossRef]
49. Morgado, E.; Mora-jiménez, I.; Vinagre, J.J.; Ramos, J.; Caamaño, A.J. End-to-End Average BER in Multihop Wireless Networks over Fading Channels. *IEEE Trans. Wirel. Commun.* **2010**, *9*, 2478–2487. [CrossRef]
50. Nistazakis, H.E.; Stassinakis, A.N.; Sheikh Muhammad, S.; Tombras, G.S. BER Estimation for Multi-Hop RoFSO QAM or PSK OFDM Communication Systems over Gamma Gamma or Exponentially Modeled Turbulence Channels. *Opt. Laser Technol.* **2014**, *64*, 106–112. [CrossRef]